Analysis of nitrogen saturation potential in Rocky Mountain tundra and forest: implications for aquatic systems

JILL S. BARON[1,2], DENNIS S. OJIMA[1],
ELISABETH A. HOLLAND[3] and WILLIAM J. PARTON[1]
[1] *Natural Resource Ecology Laboratory, Colorado State University, Fort Collins, CO 80523;* [2] *National Biological Survey;* [3] *National Center for Atmospheric Research, Boulder, CO 80307, USA*

Abstract. We employed grass and forest versions of the CENTURY model under a range of N deposition values (0.02–1.60 g N m^{-2} y^{-1}) to explore the possibility that high observed lake and stream N was due to terrestrial N saturation of alpine tundra and subalpine forest in Loch Vale Watershed, Rocky Mountain National Park, Colorado. Model results suggest that N is limiting to subalpine forest productivity, but that excess leachate from alpine tundra is sufficient to account for the current observed stream N. Tundra leachate, combined with N leached from exposed rock surfaces, produce high N loads in aquatic ecosystems above treeline in the Colorado Front Range. A combination of terrestrial leaching, large N inputs from snowmelt, high watershed gradients, rapid hydrologic flushing and lake turnover times, and possibly other nutrient limitations of aquatic organisms constrain high elevation lakes and streams from assimilating even small increases in atmospheric N. CENTURY model simulations further suggest that, while increased N deposition will worsen the situation, nitrogen saturation is an ongoing phenomenon.

1. Introduction

The availability of nitrogen in aquatic ecosystems is tightly linked with terrestrial processes of the surrounding catchment. Recent studies in eastern North America and northern Europe have documented increased stream N concentrations that appear to be strongly correlated with increased N deposition (Grennfelt & Hultberg 1986; Henriksen & Brakke 1988; Stoddard 1991). These authors and others have hypothesized a decrease in the capacity of terrestrial systems to retain nitrogen as a result of long-term N loading from atmospheric deposition (Ågren & Bosatta 1988; Aber et al. 1989). This decrease in capacity, termed nitrogen saturation, occurs when the supply of nitrogen to terrestrial ecosystems exceeds demand, and the excess N spills into aquatic ecosystems (Aber et al. 1989; Stoddard 1994). Recent N amendment experiments lend credence to this hypothesis: stream N concentrations increased markedly within a year of N applications to a watershed in the Northeast United States (Kahl et al. 1993).

We have measured surface water NO_3 concentrations in the Loch Vale Watershed in the Colorado Front Range for the past 10 years. Whereas median NO_3 concentrations for the Western Lake Survey are 0.4 μeq L^{-1} (25 μg L^{-1}; Landers et al. 1987), annual mean NO_3 concentrations at the outlet to The Loch, the lowest lake in Loch Vale Watershed are 16 μeq L^{-1} (992 μg L^{-1}), and range from values less than 1.0 μeq L^{-1} (62 μg L^{-1}) during the winter and early spring periods to 31 μeq L^{-1} (1,922 μg L^{-1}) during the peak snowmelt period (Baron 1992). High NO_3 concentrations have been observed in all seasons, and in all lakes and streams of the basin.

The Front Range is directly west of the Denver urban corridor of approximately two million people. Aged urban pollution in the form of nitrate aerosols is frequently detected at high elevations in the Front Range, and traced back to urban Denver (Heubert et al. 1983; Parrish et al. 1986, 1990). Additionally, rich agricultural lands and livestock feedlots contribute ammonia-enriched air masses to the Front Range (Langford & Fehsenfeld 1992). These nitrogen sources combine to deliver wet nitrogen deposition far in excess of what are considered background N deposition values of about 0.02 g m^{-2} (Galloway et al. 1982). Annual wet NO_3-N and NH_4-N deposition at Loch Vale Watershed averaged 0.16 (s = 0.04) and 0.10 (s = 0.03) g m^{-2}, respectively, for the eight years 1984–1991 (NADP/NTN 1993). Since some authors have reported dry deposition of up to twice the measured wet deposition, total N inputs could run as high as 0.5 g m^{-2} (Lovett & Lindberg 1984; Sievering et al. 1992).

Terrestrial processes that affect nitrogen uptake and retention are complex. Physical constraints on the ability of an ecosystem to retain nitrogen can occur where water is limiting, or where the availability of nitrogen is temporally disjunct from the growing season. This latter condition can occur in steep, snowmelt dominated systems where much of the total annual N flux occurs during early snowmelt periods (Dillon & Molot 1990; Caine 1989; Williams et al. 1993). Additionally, soil type, disturbance frequency, and age and type of vegetation affect the ability of a terrestrial ecosystem to retain N (Ågren & Bosatta 1988; Boring et al. 1988; Vitousek & Howarth 1991). The extent that other nutrients are limiting will influence the ability of terrestrial systems to retain N (Boring et al. 1988; Vitousek &Howarth 1991).

The purpose of this paper is to explore terrestrial ecosystem processes that affect nitrogen fluxes in alpine and subalpine ecosystems. Alpine tundra and subalpine forest processes were simulated with the CENTURY model for a range of N deposition values (Parton et al. 1987, 1988, 1993; Sanford et al. 1991). The simulated relative contribution to stream N loads from each vegetation type was compared with observed conditions from the Loch Vale Watershed (LVWS). Since much of LVWS has no vegetation cover at all, we do not wish to imply causality. Instead, the model results are used to explore

Fig. 1. a) Map of Colorado, showing location of the major metropolitan areas along the eastern side of the mountains. Shaded area shows elevations greater than 2800 m. Numbers on map represent total annual N deposition, in kg ha^{-1} y^{-1}, for the National Atmospheric Deposition Program sites in Colorado (NADP 1993). b) shows the study site, Loch Vale Watershed, in Rocky Mountain National Park. Hatched areas are alpine tundra, the area within the dotted line is forested, and the remaining area is bedrock or talus.

the possibility that N saturation of terrestrial and aquatic alpine and subalpine ecosystems is occurring in the Colorado Rocky Mountains.

2. Methods

2.a. *Study site*

Loch Vale Watershed is a 7 km^2 basin that drains northeast off the Continental Divide in Rocky Mountain National Park, Colorado (Fig. 1). Biogeochemical and hydrologic processes have been studied with LVWS since 1983 (Baron 1992; Denning et al. 1991). Fifty-five percent of the surface area is exposed bedrock outcrop; another 26% is talus fields where large boulders are interspersed with tundra underlain by thin, minimally developed Entisols (Walthall 1985). Alpine tundra is physically separated above the rest of the watershed by steep valley walls and covers 11% of the surface area. The remainder of the land surface is glaciers and lakes (2%), well-developed forested soils (5%), and alluvial and bog soils located in saturated areas and adjacent to streams (1%; Walthall 1985). The forest is old-growth Englemann spruce-subalpine fir ranging 200–500 years in age (Arthur & Fahey 1992). Lakes within LVWS are small (1–5 ha) and shallow (~4–7 m), with short residence times. During the April–June snowmelt period residence times range 6–39 days; during the rest of the year this lengthens to 16–105 days. Strong winds, rapid flushing,

Table 1. Mean monthly precipitation (cm), minimum and maximum air temperature (Tmin and Tmax, °C) for the forested part of Loch Vale Watershed (10-yr record, Baron 1992), and alpine Niwot Ridge (25-yr record, Greenland 1989).

	Loch Vale Watershed		
	Precipitation cm	Tmin °C	Tmax °C
Jan	6.9 (3.5)	−10.9 (1.7)	−2.9 (2.0)
Feb	8.5 (6.8)	−10.3 (1.4)	−1.6 (2.0)
Mar	13.8 (5.1)	−8.3 (2.2)	2.0 (2.4)
Apr	12.8 (3.7)	−5.0 (2.0)	6.6 (3.1)
May	9.3 (2.2)	−0.5 (1.5)	11.2 (2.0)
Jun	6.7 (3.1)	4.2 (1.1)	16.3 (2.0)
Jul	8.0 (2.5)	7.7 (2.0)	19.5 (1.5)
Aug	6.5 (2.2)	7.6 (2.6)	18.7 (1.8)
Sep	8.3 (4.5)	3.7 (2.4)	14.1 (2.8)
Oct	8.9 (7.5)	−1.3 (1.8)	7.7 (2.1)
Nov	11.3 (9.0)	−7.4 (1.5)	0.2 (1.9)
Dec	7.5 (4.7)	−10.5 (2.7)	−2.0 (3.9)

	Niwot Ridge		
	Precipitation cm	Tmin °C	Tmax °C
Jan	11.6 (6.3)	−16.7 (2.0)	−10.2 (1.9)
Feb	8.6 (3.3)	−16.4 (2.7)	−9.9 (2.1)
Mar	12.6 (4.5)	−14.8 (2.1)	−7.6 (2.2)
Apr	11.8 (5.5)	−10.5 (2.3)	−3.2 (2.7)
May	10.1 (4.0)	−5.2 (2.0)	2.2 (2.2)
Jun	5.4 (4.0)	0.4 (2.0)	8.7 (2.4)
Jul	5.8 (3.4)	3.8 (1.5)	12.0 (1.7)
Aug	5.3 (2.5)	3.1 (1.5)	10.8 (1.6)
Sep	5.0 (2.5)	−1.2 (1.8)	6.5 (1.8)
Oct	6.0 (3.6)	−6.7 (2.6)	−0.2 (2.8)
Nov	10.8 (5.9)	−13.2 (2.1)	−6.7 (2.0)
Dec	9.2 (5.1)	−16.9 (3.1)	−10.3 (2.7)

and shallow depths prevent thermal stratification during the 5 months of open water each year (Baron 1992).

Mean annual temperature is 1.5 °C, with January mean minimum and maximum temperatures of −10.9 and −2.9°C, respectively, and July mean

minimum and maximum temperatures of 7.7 and 19.5 °C, respectively (Table 1). Of the approximately 110 cm precipitation per year, 65–80% occurs as snow. Winter precipitation at the weather station is highly under-measured, due to inefficient snow capture by Belfort gages (Goodison et al. 1981), and unmeasured snow blowing into the basin from tundra surfaces to the west (Baron 1992). Measured precipitation is therefore differentiated from augmented precipitation where winter precipitation was amended by 20% to account for the additional moisture (Baron 1992). Evapotranspiration is approximately 44 cm (Baron 1992).

2.b. *Simulations*

2.b.1. *Initialization parameters*
The CENTURY model was used to simulate terrestrial processes that influence nitrogen dynamics (Parton et al. 1987, 1988, 1993; Sanford et al. 1991). CENTURY is a general model of plant-soil ecosystems that represents carbon and nutrient dynamics. Within CENTURY, plant production submodels are linked to a common soil organic matter (SOM) submodel that simulates the flow of elements through the different organic and inorganic pools in the soil. Soil carbon (C) is divided into three major components that include active, slow and passive soil C. Active SOM includes live soil microbes plus microbial products, the slow pool includes resistent plant materials (such as lignin-like components), and soil-stabilized plant and microbial material, and the passive material includes physically and chemically stabilized SOM that is very resistent to decomposition. Since CENTURY has been previously described in detail (Parton et al. 1987, 1988, 1993; Sanford et al. 1991), only the nitrogen and water submodels will be elaborated on below. Ecological input variables include soil N inputs, initial soil C and N levels, soil pH and texture, lignin content of plant material (for the forest version), and plant N content.

Tundra simulations were conducted using the grass plant production submodel (Parton et al. 1993) that was initialized with tundra values from Webber & May (1977). Nitrogen fluxes were parameterized to reflect field experimental results for N-fixation from Bowman et al. (1993a) and for N volatilization rates from S.K. Schmidt (personal communication). The temperature function for microbial decomposition was modified from the original grass model. Temperature was derived from soil collected at Niwot Ridge and incubated at 5, 10, 15, 25 and 35 °C (Cleveland et al. 1993). Soil water content of the samples was brought to field capacity before incubation. Microbial activity was calculated as the CO_2 respired during the first 24 hours of incubation for a given temperature divided by CO_2 respired during the first 24 hours of incubation at 35 °C (the maximum). We then fit a generalized
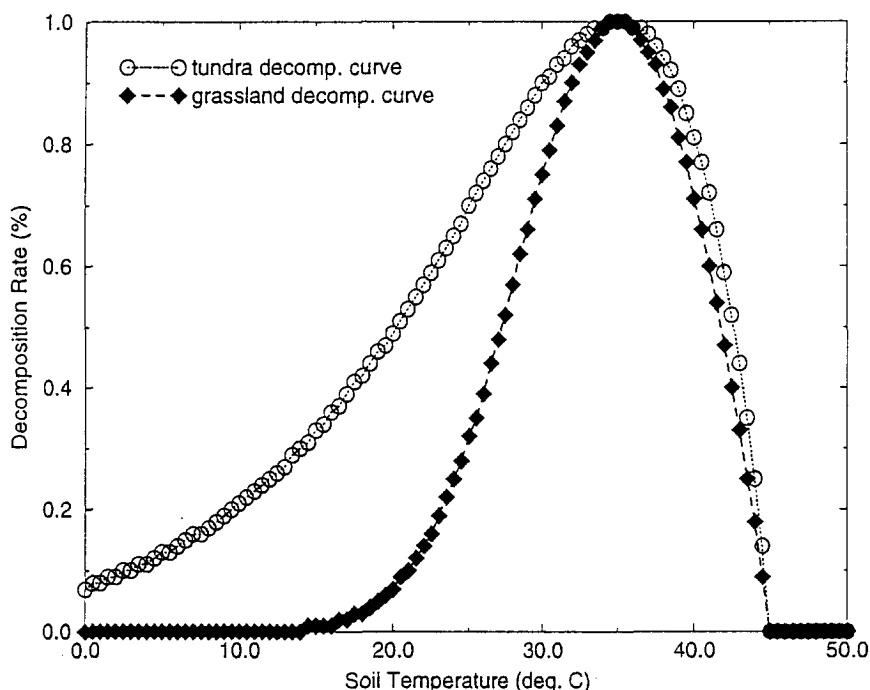
Fig. 2. The effect of soil temperature on decomposition rates in the CENTURY model. The circles show the modification for tundra soils determined from laboratory incubations (Cleveland et al. 1993). The diamonds represent the standard temperature:decomposition relation used in CENTURY.

poisson density function to the data assuming an optimum temperature of 35 °C, and that microbial activity declined to zero at a maximum temperature of 45 °C. The curve fitting was done using the nonlinear fitting routine provided in SYSTAT (SYSTAT for the Macintosh, version 5.2, SYSTAT 1992). The fitting routine defined the shape parameters to the left and right of the optimum temperature for decomposition, so that left shape parameter = 1.236 (compared with 2.63 in a lower elevation grassland), and the right shape parameter stayed the same as lower elevation grasslands at 0.9 (Fig. 2).

Forest simulations used the forest plant production submodel (Sanford et al. 1991). In the forest version of CENTURY, a plant production submodel that allocates carbon to leaves, fine roots, fine branches, large wood, and coarse roots, was linked to a soil organic matter submodel (Sanford et al. 1991). Initialization values were taken from Arthur & Fahey (1992). Nitrous oxide flux values from control plots of a New Mexico coniferous forest study were used to initialize N volatilization rates (Matson et al. 1992).
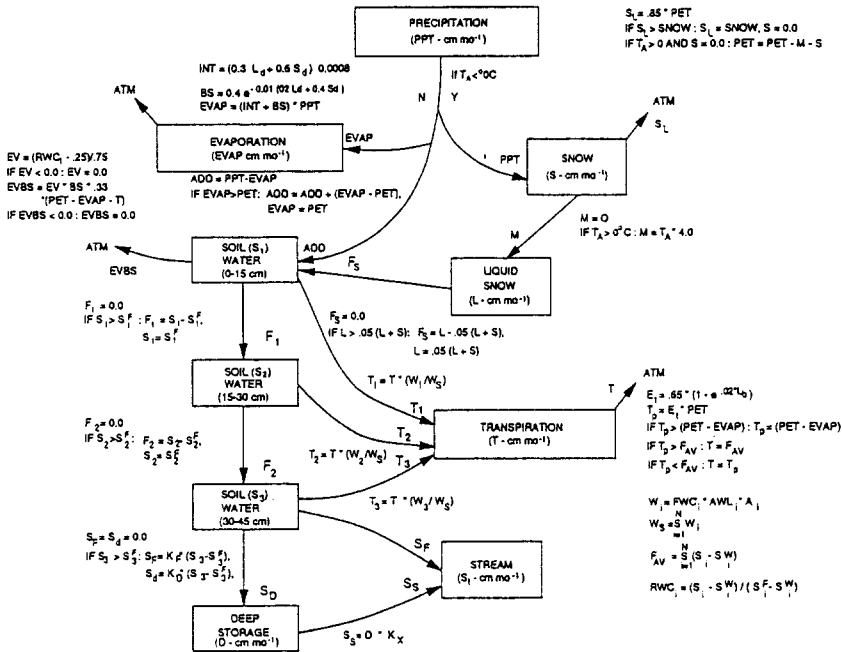
Fig. 3. Flow diagram of the water submodel in CENTURY. Variable terms are identified in Table 2 (Parton et al. 1993).

CENTURY runs with a monthly time step, and requires meteorological inputs of mean monthly precipitation, minimum and maximum air temperature (Table 1). Soil texture, horizon depths and bulk density data were taken from May & Webber (1982) for the tundra, and from Arthur (1990) and Walthall (1985) for the forest.

2.b.2. *Water submodel description*
The CENTURY model includes a simplified water budget model that calculates monthly evaporation and transpiration water loss, water content of the soil layers, snow water content and saturated flow of water between soil layers (Fig. 3, Table 2). If the average air temperature is less than 0 °C, then monthly precipitation occurs as snow. Sublimation and evaporation of water from the snow pack occurs at a rate equal to the potential evapotranspiration rate. Snow melt occurs if the average air temperature is greater than 0 °C and is a linear function of the average air temperature. The potential evapotranspiration rate (PET) is calculated as a function of the average monthly maximum and minimum air temperature using the equations developed by Linacre (1977). Bare soil water loss is a function of standing dead and litter biomass (lower for high

Table 2. Definitions of variables used in the CENTURY water flow submodel (see Fig. 3). For detailed validations and descriptions, refer to Parton et al. (1993).

ADD	water added to the soil (cm mo^{-1}).
A_i	depth of ith layer (cm).
ATM	atmospheric H_2O sink or source (cm).
AWL_i	relative root density in the i layer (0–1).
BS	fraction of PPT lost as bare soil H_2O loss (0–1).
D	deep H_2O storage (cm).
E_t	fraction of H_2O loss by transpiration (0–1).
EVAP	bare soil plus interception H_2O loss (cm).
EVBS	bare soil evapotranspiration (cm mo^{-1}).
F_{AV}	total H_2O available for transpiration H_2O loss (cm).
F_i	saturated H_2O flow from i layer to the i + 1 layer (cm mo^{-1}).
INT	fraction of PPT lost as interception H_2O loss (0–1).
K_d	fraction of excess H_2O flowing to D_S (0–1).
K_F	fraction of excess H_2O flowing to S_F (0–1).
K_X	fraction of D flowing to S_F.
L	liquid snow pack (cm).
L_b	aboveground live plant biomass (g m^{-2}).
L_d	surface litter biomass (g m^{-2}).
M	the H_2O melting from S (cm mo^{-1}).
N	the number of soil layer units with roots
PET	potential evapotranspiration H_2O loss (cm).
PPT	monthly precipitation (cm mo^{-1}).
RWC_i	the relative water content for the ith layer.
S	frozen snow pack (cm).
S_d	standing dead plus live plant biomass (g m^{-2}).
S_D	saturated drainage to deep storage (cm mo^{-1}).
S_F	stream flow (cm mo^{-1}).
S_i	soil water in the ith layer (cm).
S_i^F	field capacity of i layer (cm).
S_i^W	wilting point of i layer (cm).
S_S	H_2O flow from D to S_F (cm mo^{-1}).
S_l	sublimation H_2O loss (cm mo^{-1}).
T	transpiration H_2O loss (cm mo^{-1}).
T_i	transpiration H_2O loss ith layer (cm mo^{-1}).
T_P	potential transpiration H_2O loss (cm mo^{-1}).
W_i	weight factor for transpiration H_2O loss from the ith layer (0–1).

biomass levels), rainfall, and PET. The interception water loss is a function of aboveground biomass (increases with biomass level), rainfall, and PET. Transpiration water loss is function of the live leaf biomass (exponential function
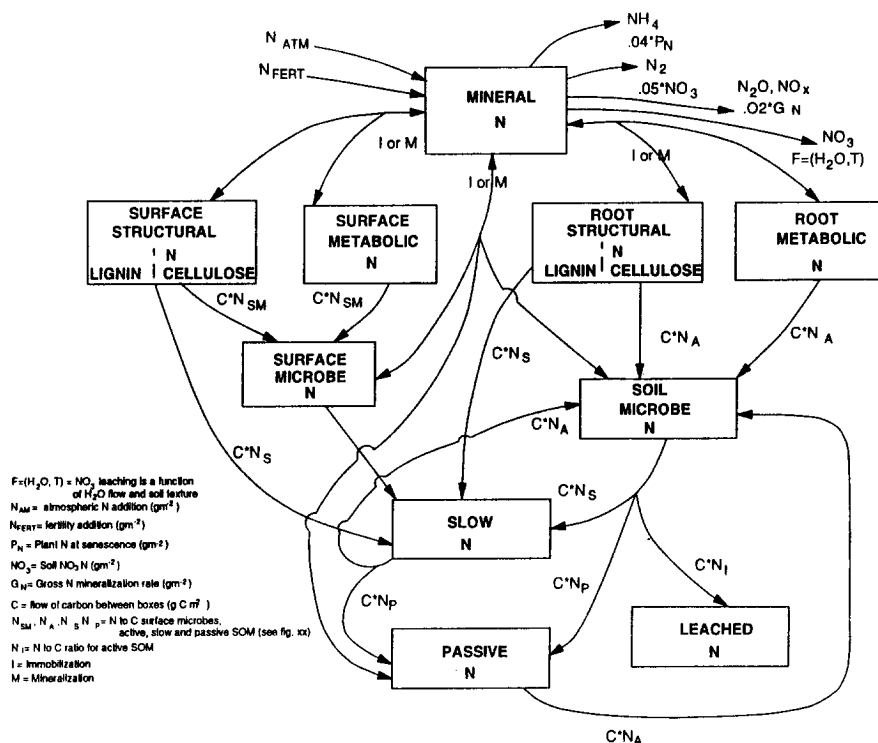
Fig. 4. Flow diagram of the nitrogen submodel in CENTURY. The submodel is described generally in the text, and described in detail in Parton et al. 1987, 1988, 1993.

of leaf biomass), rainfall, and PET. Interception of water and bare soil water losses are calculated as fractions of the monthly precipitation and are subtracted from the total monthly precipitation. The remainder of precipitation water is added to the soil.

Water is distributed to the different layers by adding the water to the top layer (0–15 cm) and then draining excess water (water above field capacity) to the next layer. Transpiration water loss occurs after the water was added to the soil. Water loss occurs first as interception, followed by bare soil evaporation and transpiration (the sum does not exceed the PET rate). The field capacity and wilting point for the different soil layers is calculated as a function of the bulk density, soil texture, and organic matter content using equations from Gupta & Larson (1979). The number of soil layers is an input variable in the model, and we used 15-cm increments for each layer up to the 60-cm soil depth and 30-cm increments below the 60-cm depth. Water leached below the last soil layer is lost as stream flow. Some additional detail is provided in Parton et al. (1993).

2.b.3. *Nitrogen submodel*

The N submodel (Fig. 4) has the same general structure as the soil carbon (C) model that is described in detail in Parton et al. (1987, 1988, 1993). Organic-N flows follow C flows and are equal to the product of the carbon flow and the C:N ratio of the state variable that receives the C. The C:N ratios of the soil state variables receiving the flow of C are a function of the mineral N pool (NO_3 plus NH_4). These ratios vary within the ranges 3–15, 12–20, and 7–10, respectively, for active, slow and passive soil organic matter (SOM) turnover pools. Nitrogen associated with carbon lost in respiration is assumed to be mineralized. Decomposition of metabolic residue and the active, slow, and passive pools generally results in net mineralization of N. Decomposition of structural material immobilizes N. The model also uses simple equations to represent N inputs due to atmospheric deposition and N fixation and calculates N losses due to N_2, NO, N_2O, and NH_3 gas fluxes (see Fig. 4) and NO_3 leaching.

Leaching of labile mineral N (NO_3 and NH_4) occurs when saturated water flows between soil layers. The fraction of mineral N that flows from the upper layer to the lower layer is calculated as a function of the sand content of the soil and the amount of saturated water flow between layers (Fig. 4). Parameter values were determined by fitting the model to observed water chemistry data (McDowell & Asbury 1994).

Nitrogen dynamics were simulated by running the model for a range of 0.02–1.6 g N deposition m^{-2} y^{-1}. For each deposition rate, 1060 year runs were made with CENTURY for each vegetation type, the tundra and the forest. This time period was sufficient to bring all processes to equilibrium at the specified deposition rate. Averages of the last 60 years were used in analyses below.

3. Results

3.a. *CENTURY model results: terrestrial processes*

The thousand-year runs allowed ecosystem dynamics, including plant and soil organic matter processes, to equilibrate for each deposition amount. Compartments and flux rates for the range of current deposition (0.3–0.6 g N m^{-2} y^{-1}) show that most of the tundra biomass was belowground (Table 3a). Total forest biomass was somewhat greater than tundra, and was allocated primarily to aboveground wood and needles. Much more N was stored in tundra plant material than in forest material. Approximately equal amounts of C and N were labile in both tundra and forest, and this was only 3–5% of the total SOM pools for these elements. Total plant C production was similar between the two vegetation types, while N uptake was 20–30% greater in the

Table 3. Simulated ecosystem compartments (a) and fluxes (b) of 0.3 and 0.6 g N m^{-2} y^{-1} deposition. Values are mean and (std. dev.) of last 10 years of a 1060 year simulation.

A. Ecosystem components (g m^{-2})

| | Plant material | | | | Soil organic matter | | | |
| | C | | | N | C | | N | |
	Aboveground	Belowground	Total	Total	Labile	Total	Labile	Total
Tundra 0.3	19 (30)	5,600 (360)	5,619 (390)	108 (9)	340 (70)	10,000 (230)	52 (7)	960 (8)
Tundra 0.6	21 (33)	6,271 (402)	6,292 (435)	123 (8)	379 (76)	10,806 (260)	60 (8)	1,030 (10)
Forest 0.3	6194 (33)	1,030 (10)	7,224 (43)	28 (0)	289 (2)	7,918 (14)	20 (0)	592 (0)
Forest 0.6	8940 (42)	1,440 (8)	10,380 (50)	40 (0)	413 (4)	10,613 (21)	33 (0)	782 (0)

B. Ecosystem processes (g m^{-2} y^{-1})

| | Plant C production | | | Net mineralization | Plant uptake | N dynamics | |
	Aboveground	Belowground	Total			Volatilization	Excess inorganic (leached)
Tundra 0.3	100 (23)	111 (29)	211 (52)	3.7 (0.8)	3.7 (0.9)	0.0001 (0.000)	0.2 (0.2)
Tundra 0.6	112 (22)	124 (27)	236 (49)	3.9 (0.8)	4.5 (1.3)	0.0001 (0.000)	0.2 (0.2)
Forest 0.3	130 (20)	63 (10)	193 (31)	2.0 (0.4)	2.1 (0.4)	0.048 (0.003)	0.002 (0.001)
Forest 0.6	191 (11)	90 (5)	281 (16)	2.8 (0.3)	3.1 (0.3)	0.089 (0.005)	0.08 (0.05)

tundra than in the forest (Table 3b). N mineralization and leaching rates were greater in tundra than in forest, but more N was volatilized from forest than tundra.

Model output for the range of current N deposition (0.3–0.6 g N m^{-2} y^{-1}) was compared with measured values from forest and tundra systems (Table 4). Tundra runs were initialized with data reported in 1977 by Webber and May, so we compared them with more recent values (Bowman et al. 1993b, Walker et al. 1994). Because Loch Vale Watershed data were used to initialize CENTURY forest runs, we compare model output with findings from other, similar, sites. While this does not constitute true model validation, it places our results within reasonable boundaries. Because N mineralization rates are a calculated product of the model, we compared them with measured LVWS values.

There was very good agreement between simulated and observed values for average annual C production (the sum of above- and belowground C accumulation) and soil organic matter carbon in both tundra and forest. The simulated values of aboveground C production were narrower than those observed by Bowman et al. (1993b) and Walker et al. (1994), while simulated belowground live C was slightly higher than observed values (Bowman et al. 1993). More N mineralization was simulated than was actually measured on Niwot Ridge by Bowman et al. (1993b), but the simulated values fell within those measured in several European tundra systems (Rehder 1976; Gökçeoğlu & Rehder 1977; Rehder & Schafer 1978). Soil organic matter C, which was somewhat higher in tundra than in forest, compared favorably with recent measurements by Walker et al. (1994) and Neff (in prep.).

Forest C production was similar to that observed in a spruce-fir forest system in Alberta (Prescott et al. 1989). Simulated N mineralization rates were slightly lower than observed in LVWS (Arthur 1990; Arthur & Fahey 1992). Simulated soil organic matter carbon values were very close to measured values from a number of studies (Cole & Rapp 1981; Vogt et al. 1986; Prescott et al. 1989).

Tundra ecosystem processes responded only slightly to increases in N deposition (Fig. 5). Annual production (above- and belowground) did not increase until deposition reached 0.1 g N m^{-2} y^{-1}. Subsequent productivity increases were slight, increasing from 90 to 125 g C m^{-2} y^{-1} as the deposition increased more than an order of magnitude from 0.1 to 1.6 g N m^{-2} y^{-1}. Mineralization rates responded only slightly when N deposition reached a rate of 0.1 g N m^{-2} y^{-1}, increasing from 3.4 to slightly less than 4.3 g N m^{-2} y^{-1}. The largest response to increased N deposition to the tundra occurred in soil organic matter, where gains of 2,000 g C and 200 g N m^{-2} were simulated.

Table 4. Modeled and observed values for plant productivity and ecosystem parameters. Simulated forest and tundra values are presented for the deposition range of 0.3–0.6 g N m^{-2}. Tundra initialization values are from Webber & May (1977). Forest runs were initialized with data from Arthur & Fahey (1992). Aboveground biomass values from the literature were multiplied by 0.45 to convert to g C. Bulk density for the tundra was 0.9. Measurements and simulations report soil organic matter to 20 cm depth. Values in parentheses are standard errors.

Parameters	Initialization values	Simulated tundra	Observed tundra
Aboveground C production (g m^{-2} y^{-1})	40–125	100–112	70–135 (Bowman et al. 1993) 43–107 (Walker et al. 1994)
Belowground live C (g m^{-2})	1,000–5,000	4,900–5,570	2,250–4,200 (Bowman et al. 1993)
Annual net N mineralization (g m^{-2} y^{-1})	not an input	3.7–3.9	~2.0 (Bowman 1992) 0.14–5.0 (Rehder 1976; Gökçeoğlu & Rehder 1977; Rehder & Schafer 1978)
Total soil organic matter carbon (g m^{-2})	5,000–15,000	10,000–10,806	13,500–39,600, ave. 25,294 (J. Neff, pers. comm.)

| Parameters	Initialization values	Simulated forest	Observed forest
Forest C production (g m^{-2} y^{-1})	137–344	197–282	200 (Prescott et al. 1989)
Annual net N mineralization (g m^{-2} y^{-1})	not an input	2.1–2.8	2.0–3.0 (Arthur 1990; Arthur & Fahey 1992)
Total soil organic matter carbon (g m^{-2})	5,650–7,000	7,900–10,700	5,700 (Prescott et al. 1989) 7,500 (s.e. = 2,700) (Cole & Rapp 1981) 4,500 (s.e. = 2,700) (Vogt et al. 1986)
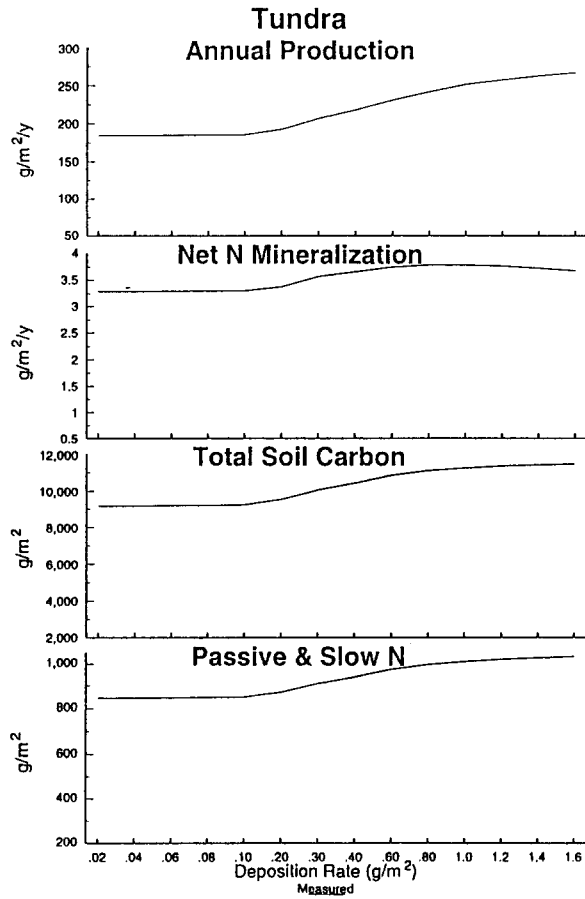
Fig. 5. CENTURY model results of 1060 year simulations of tundra processes at increasing N deposition loads. Annual production of above- and belowground carbon (C), and net nitrogen (N) mineralization are shown as rates, in g m^{-2} y^{-1}. Total soil C and that N stored in passive and slow soil organic matter (SOM) are shown as pools, in g m^{-2}.

Again, rates of SOM accumulation increased when deposition increased to 0.1 g N m^{-2} y^{-1} and greater.

The response of the forest system to increased N deposition was more pronounced than the tundra response (Fig. 6). Forest annual production increased five times with the increase in available N from deposition, from 60 to 280 g C m^{-2} y^{-1}. Net N mineralization rates increased three times, from 0.79 to 2.73 g N m^{-2} y^{-1}. Soil organic matter C and N increased between two and threefold, increasing from about 5,500 g C m^{-2} y^{-1} and 320 g N m^{-2} y^{-1} to nearly 11,000 g C m^{-2} y^{-1} and 820 g N m^{-2} y^{-1}. As with tundra, the greatest increases in forest process response occurred at N deposition rates
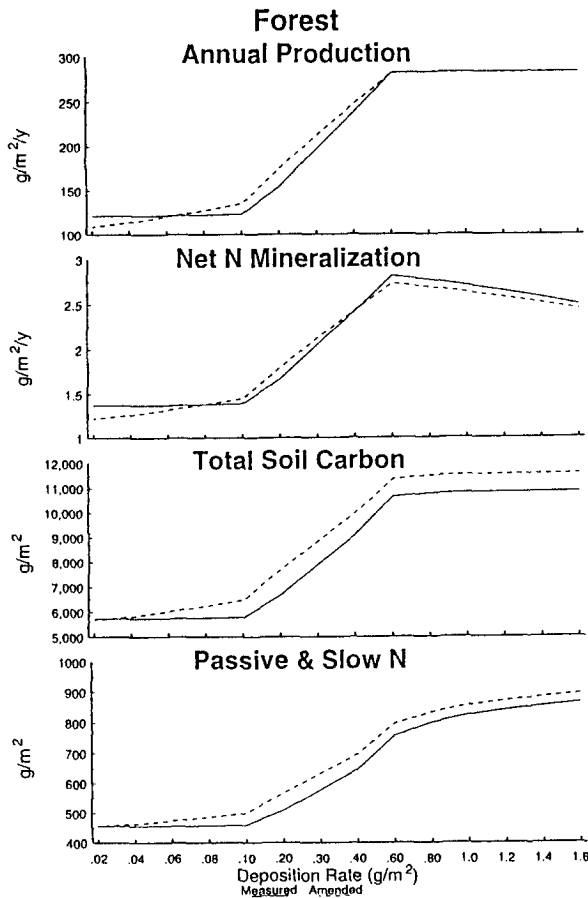
Fig. 6. CENTURY model results of 1060 year simulations of forest processes at increasing N deposition loads. Annual carbon production, g m^{-2} y^{-1}, is the sum of fine and coarse root, fine branch, coarse wood, and leaf production. Net nitrogen (N) mineralization is in g m^{-2} y^{-1}. Total soil C and the N stored in passive and slow soil organic matter (SOM) are shown as pools, in g m^{-2}.

greater than 0.1 m^{-2} y^{-1}. Increased (amended) precipitation had little effect on forest processes, although there was a slight increase in soil organic matter C and N.

3.b. *CENTURY model results: stream dynamics*

Monthly stream discharge for both tundra and forest approximated actual discharge, in that peak flows occurred June–August (Fig. 7a). Simulated chemical fluxes also followed discharge patterns (Fig. 7b). Almost all efflux of nitrogen from LVWS occurred during the snow melt period (April–July)
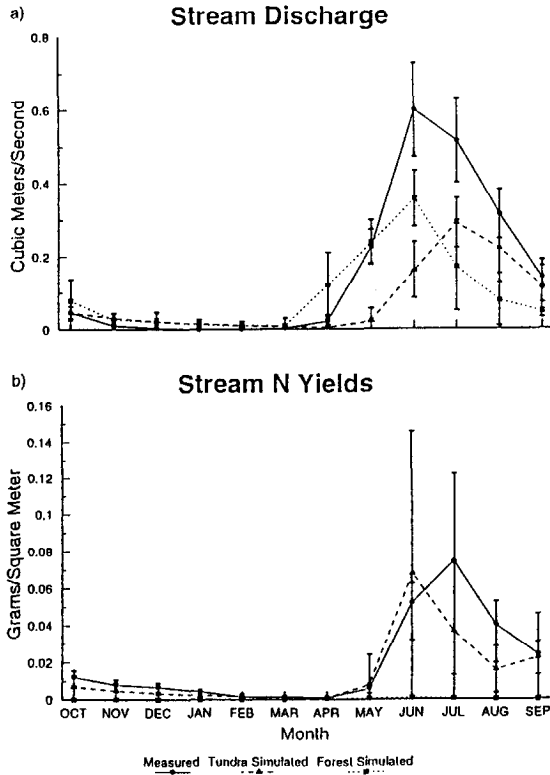
Fig. 7. Mean monthly observed and simulated stream a) discharge (m^3 s^{-1}) and b) N yield (g m^{-2}) from Loch Vale Watershed. Data are 10-yr averages (1983–1992). Tundra and forest simulations are 60-yr average values from the last 60 years of a 1060-yr CENTURY model run.

of each year. No direct comparison of simulated versus observed stream discharge or chemistry was made for two reasons: the watershed is a complex mix of tundra, forest, and bedrock, and CENTURY is a point model that doesn't lend itself to spatial analysis.

Stream N values were dominated by leachate from tundra (Fig. 8). According to the model, tundra was unable to assimilate all of the available N even when deposition was extremely low. At depositions below 0.2 g N m^{-2} y^{-1} losses from tundra were steady at 0.1 g N m^{-2} y^{-1}. Nitrogen losses from the tundra system increased as deposition increased above 0.2 g N m^{-2} y^{-1}. The N mass balance (ratio of inputs:outputs) decreased from greater than 1.0 where depositions are 0.1 g N or less, to less than 1.0 at higher depositions. The input:output ratio stabilized at 0.32 at deposition values greater than 1.0 g N m^{-2} y^{-1}. Forest leachate increased rapidly at depositions greater than 0.4 g N m^{-2} y^{-1}, and could account for more than half the observed stream N
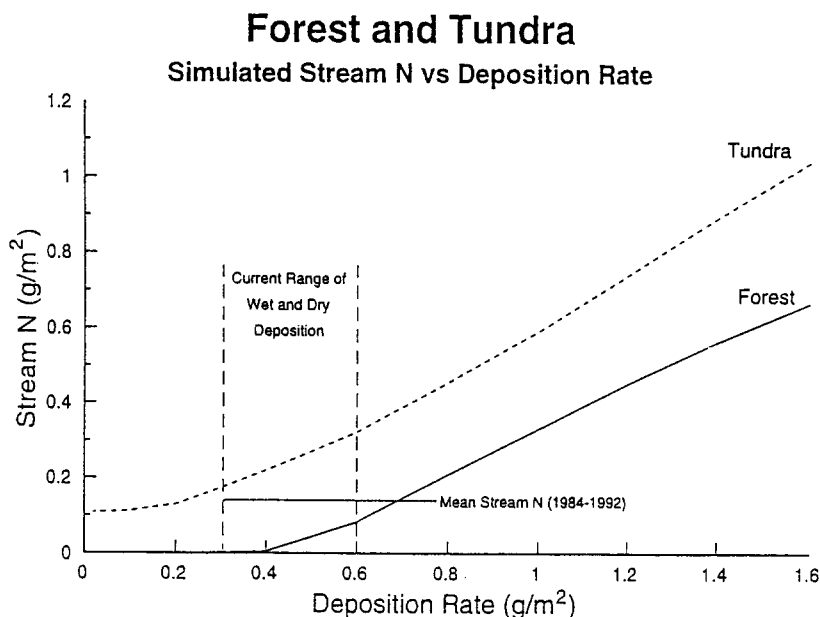
Forest and Tundra
Simulated Stream N vs Deposition Rate

Fig. 8. CENTURY model results of stream responses to tundra and forest processes under a range of N deposition scenarios, from 0.02–1.6 g N m^{-2} y^{-1}. The current range of N deposition values, from 0.3 g N m^{-2} y^{-1} measured as wet deposition in Loch Vale Watershed, to 0.6 g N m^{-2} y^{-1}, if dry deposition is equal to that measured, is shown within the dashed bars. The mean observed stream N yield during 1984–1992 of 0.15 g N m^{-2} y^{-1} is shown as a line within the dashed deposition bars.

values when deposition was 0.6 g N m^{-2} y^{-1}. Some N was always retained by the forest system, however; N losses did not exceed inputs even at the highest deposition rates.

4. Discussion

4.a. *Terrestrial responses to N deposition*

Tundra processes responded slightly to increasing N deposition, but appeared to be strongly limited by other factors in the CENTURY simulations. These results are supported by recent research on tundra primary production (Bowman et al. 1993b) and the importance of climate (Walker et al. 1994). While large N amendments (25 g N m^{-2} y^{-1}) to dry and wet alpine meadows of Niwot Ridge, Colorado, produced an increase in total above ground biomass, the increase was due to changes in community structure. Individual plant response to increased nutrient availability was not changed from control plots, so Bowman et al. (1993b) suggest current alpine tundra communities are adapted to low nutrient availability. Plant composition in CENTURY is

fixed, so could not reflect a shift in community structure in response to changing N availability. The model strongly suggests, however, as do Bowman et al.'s experimental data, that other factors than N control tundra plant productivity. The model further suggests that above 0.2 g N m^{-2} y^{-1} nitrogen is no longer limiting to plant growth, since that is the deposition above which N leaching increases. Walker et al. (1994) found climate factors to account for 15–40% of above ground biomass.

The CENTURY results suggest forest microbial and vegetation processes are limited by N, but may currently be undergoing fertilization-induced rate increases. Limitations are supported by observations from Loch Vale Watershed, where mean NO$_3$ concentrations in forest floor and B horizon lysimeters were less than 10 μeq L^{-1} (620 μg L^{-1}; Denning et al. 1991; Arthur & Fahey 1993). Further research is necessary to verify model results.

4.b. *Aquatic implications*

Simulated tundra leachate at deposition values that bracket the current N deposition rates ranged 0.2–0.3 g N m^{-2} y^{-1}. This is more than enough to account for the currently observed stream N shown in Fig. 8. Considering that only 11% of the Loch Vale Watershed is vegetated with tundra, and another 81% is exposed bedrock or talus, elevated nitrogen deposition has serious implications for alpine aquatic ecosystems. The N lost from tundra to stream increased linearly with increasing deposition above the simulated deposition rates of 0.6 g N m^{-2} y^{-1}. Roughly 30% of the inputs was retained by the tundra community. Leaching off rock areas is expected to add even more N to alpine streams because these offer even fewer opportunities for sequestering nitrogen.

While simulated forest leachate was less than the current measured values of stream N, forest leachate, too, increases with increased deposition. This suggests subalpine streams may also be at risk from increasing rates of N deposition.

The fraction of the annual N load stored in snowpacks, and the pathway by which it reaches the stream system, further affects aquatic nitrogen dynamics. In the Emerald Lake Watershed of California, 90% of the annual solute flux was associated with snowpack runoff and rainfall during snowmelt (Williams & Melack 1991). High NO$_3$ concentrations were detected in soils of Emerald Lake Watershed, and in small inlets to the lake, but NO$_3$ was virtually undetectable in the outflow from Emerald Lake itself (Williams et al. 1993; Williams & Melack 1991). In LVWS about 47% of the total annual N yield occurs during April and May (Baron 1992). This loss occurs before the onset of the tundra growing season in early to mid-June (Bowman 1992).

Snowmelt-related flux partially explains the high observed stream and lake N values.

Watershed gradient, discharge rates, and lake hydrologic retention time are important physical factors that control the contact period of N with substrates where consumption or sorption can take place in aquatic systems (Dillon & Molot 1990). In Loch Vale Watershed the overall watershed gradient is steep at 15–20%. The hydrologic retention time for the largest lake in LVWS, Sky Pond, is 0.42 y^{-1} (Baron 1992). Only during the winter period of ice-cover and minimum discharge is there evidence of N consumption within lakes and surface waters. Approximately 20% of the total Sky Pond N content is consumed in lake bottom waters by sediment microbial activity during the winter months (Baron 1992). Sediment processes are undetectable at other times of the year.

Phytoplankton consumes nitrogen under lake ice in early winter and during spring snowmelt (McKnight et al. 1990; Spaulding 1991), but lake NO_3 concentrations rarely drop below 10 $\mu eq\ L^{-1}$ (620 $\mu g\ L^{-1}$) in LVWS (Baron 1992). Many investigators have reported on phosphorous limitations to freshwater algal productivity (see Vitousek & Howarth 1991). Our work on nutrient limitations in LVWS is not definitive, but there is a suggestion from short term nutrient enrichment experiments that productivity increases were due to elements other than nitrogen, such as trace metals or phosphorous (McKnight et al. 1990). When N limitations are overcome there may be a shift in algal communities (Christie & Smol 1993; Vitousek & Howarth 1991), and eventually episodic or chronic acidification (Stoddard 1994).

5. Conclusions

Elevated levels of wet deposited N occur in the Colorado Front Range. Current deposition levels alone are sufficient to have exceeded the nitrogen demands of alpine tundra, according to the CENTURY model results. Subalpine forests appear to still be limited by N availability, although growth rates increase rapidly with increasing N inputs. Nitrogen leaching from tundra, combined with N leached from exposed rock surfaces, produce high N loads in aquatic ecosystems above treeline in the Colorado Front Range. Nitrogen loads are high in Loch Vale Watershed streams. A combination of terrestrial leaching, large N inputs form snowmelt, the high watershed gradient, rapid lake turnover time, and phosphorous limitations of aquatic organisms constrain alpine tundra streams from assimilating even small increases in atmospheric N. CENTURY model simulations further suggest that, while increased N deposition will worsen the situation, nitrogen saturation is an ongoing phenomenon.

Acknowledgements

References

Aber JD, Nadelhoffer KJ, Steudler P & Melillo (1989) Nitrogen saturation in northern forest ecosystems. BioScience 39: 378–386

Ågren GI & Bosatta E (1988) Nitrogen saturation of the terrestrial ecosystem. Environ. Pollut. 54: 185–197

Arthur MA (1990) The effects of vegetation on watershed biogeochemistry at Loch Vale Watershed, Rocky Mountain National Park, Colorado. Ph.D. Dissertation. Cornell University, Ithaca, NY

Arthur MA & Fahey TJ (1992) Biomass and nutrients in an Englemann spruce-subalpine fir forest in north central Colorado: pools, annual production, and internal cycling. Can. J. For. Res. 22: 315–235

Arthur MA & Fahey TJ (1993) Controls on soil solution chemistry in a subalpine forest in north-central Colorado. Soil Sci. Am. J. 57: 1122–1130

Baron J (1992) Biogeochemistry of a subalpine ecosystem: Loch Vale Watershed. Ecological Studies 90. Springer-Verlag, New York

Boring LR, Swank WT, Waide JB & Henderson GS (1988) Sources, fates, and impacts of nitrogen inputs to terrestrial ecosystems: review and synthesis. Biogeochemistry 6: 119–159

Bowman WD (1992) Inputs and storage of nitrogen in winter snowpack in an alpine ecosystem. Arc. Alp. Res. 24: 211–215

Bowman WD, Schardt JC, Schmidt SK & Thomas B (1993a) Symbiotic nitrogen fixation by three alpine Trifolium species. Abstract from Niwot Ridge/Green Lakes Valley Research Workshop, 21 August 1993

Bowman WD, Theodose TA, Schardt JC & Conant RT (1993b) Constraints of nutrient availability on primary production in two alpine tundra communities. Ecology 74: 2085–2097

Caine N (1989) Hydrograph separation in a small alpine basin based on inorganic solute concentrations. J. Hydrol. 112: 89–110

Christie CE & Smol JP (1993) Diatoms assemblages as indicators of lake trophic status in southeastern Ontario lakes. Jour. Phycol. 29: 575–591

Cleveland CC, Holland EA & Neff JC (1993) Temperature regulation of soil respiration in an alpine tundra ecosystem. Poster and Abstract, Front Range AGU Meeting, Golden, CO, Feb. 1993

Cole DW & Rapp M (1981) Element cycling in forest ecosystems. In: Raichle RE (Ed) International Biological Programme 23 (pp. 341–409). Cambridge University Press

Denning AS, Baron J, Mast MA & Arthur M (1991) Hydrologic pathways and chemical composition of runoff during snowmelt in Loch Vale Watershed, Rocky Mountain National Park, Colorado, USA. Water, Air, Soil Pollut. 59: 107–123

Dillon PJ & Molot LA (1990) The role of ammonium and nitrate retention in the acidification of lakes and forested catchments. Biogeochemistry 11: 23–43

Galloway JN, Likens GE, Keene WC & Miller JM (1982) The composition of precipitation in remote areas of the world. J. Geophys. Res. 87: 8771–8776

Gökçeoğlu M & Rehder H (1977) Nutrient turnover studies in alpine ecosystems. III. Communities of lower altitudes dominated by *Carex sempervirens* Vill. and *Carex ferruginea* Scop. Oecologia 28: 317–331

Goodison BE, Ferguson HL & McKay GA (1981) Measurement and data analysis. In: Gray DM & Hale DH (Eds) Handbook of Snow: Principles, Processes, Management and Use (pp. 191–274). Pergamon Press, Willowdale, Ontario

Grennfelt P & Hultberg H (1986) Effects of nitrogen deposition on the acidification of terrestrial and aquatic ecosystems. Wat. Air, Soil Pollut. 30: 945–963

Gupta SC & Larson WE (1979) Estimating soil water retention characteristics from particle size distribution, organic matter content, and bulk density. Wat. Resour. Res. 15: 1633–1635

Henriksen A & Brakke DF (1988) Increasing contributions of nitrogen to the acidity of surface waters in Norway. Wat., Air, Soil Pollut. 42: 183–201

Heubert BJ, Norton RB, Bollinger MJ, Parrish DD, Hahn C, Bush YA, Murphy PC, Fehsenfeld FC & Albritton DL (1983) Gas phase and precipitation acidities in the Colorado mountains. In: Herrmann R & Johnson AI (Eds) International Symposium on Hydrometerology (pp. 17–24). Proceedings of the American Water Resources Association, Bethesda, MD 20814

Kahl JS, Norton SA, Fernandez IJ, Nadelhoffer KJ, Driscoll CT & Aber JD (1993) Experimental inducement of nitrogen saturation at the watershed scale. Environ. Sci. Technol. 27: 565–568

Landers DH, Eilers JM, Brakke DF, Overton WS, Schonbrod RD, Crowe RT, Linthurst RA, Omernik JA, Teague SA & Meier EP (1987) Characteristics of lakes in the western United States, Vol I: Population descriptions and physicochemical relationships. EPA-6003-86/054a, US Environment Protection Agency, Washington, DC

Langford AO & Fehsenfeld FC (1992) Natural vegetation as a source or sink for atmospheric ammonia: a case study. Science 255: 581–583

Linacre ET (1977) A simple formula for estimating evaporation rates in various climates, using temperature data alone. Agric. Meteorol. 18: 409–424

Lovett GM & Lindberg SE (1984) Dry deposition and canopy exchange in a mixed oak forest as determined by analyzing throughfall. J. Appl. Ecol. 21: 1013–1023

Matson PA, Gower ST, Volkmann C, Billow C & Grier CC (1992) Soil nitrogen cycling and nitrous oxide flux in a Rocky Mountain Douglas-fir forest: effects of fertilization, irrigation and carbon addition. Biogeochemistry 18: 101–117

May DE & Webber PJ (1982) Spatial and temporal variation of the vegetation and its productivity on Niwot Ridge, Colorado. In: Halfpenny JC (Ed) Ecological Studies in the Colorado Alpine: a festschrift for John W. Marr (pp. 35–62). Occasional Paper No. 37. Institute of Arctic and Alpine Research, University of Colorado, Boulder

McDowell WH & Asbury CE (1994) Export of carbon, nitrogen, and major ions from three tropical montane watersheds. Limnol. Oceanogr. 39: 111–125

McKnight DM, Smith RL, Bradbury JP, Baron JS & Spaulding S (1990) Phytoplankton dynamics in three Rocky Mountain lakes, Colorado USA. Arctic Alp. Res. 22: 264–274

NADP/NTN (1993) National Atmospheric Deposition Program. Tape of weekly data. National Atmospheric Deposition Program (IR-7)/National Trends Network. July 1978–September 1993. [Magnetic tape, 9 track, 1600 cpi. ASCII.] NADP/NTN Coordination Office, Natural Resource Ecology Laboratory, Colorado State University, Fort Collins, CO

Parrish DD, Hahn CH, Fahey DW, Williams EJ, Bollinger MJ, Bler HG, Burh MP, Murphy PC, Trainer M, Hsie EY, Lui SC & Fehsenfeld FC (1990) Systematic variations in the concentration of NOx (NO plus NO_2) at Niwot Ridge, Colorado. J. Geophy. Res. 95: 1817–1836

Parrish DD, Norton RB, Bollinger MJ, Liu SC, Murphy PC, Albritton DL, Fehsenfled FC & Heubert BJ (1986) Measurements of HNO_3 and NO_3^- at a rural site in the Colorado mountains. J. Geophys. Res. 91: 5379-5393

Parton WJ, Schimel DS, Cole CV & Ojima DS (1987) Analysis of factors controlling soil organic matter levels in Great Plains grasslands. Soil Sci. Soc. Am. J. 51: 1173–1179

Parton WJ, Stewart JWB & Cole CV (1988) Dynamics of C, N, P, and S in grassland soils: a model. Biogeochemistry 5: 109–131

Parton WJ, Scurlock JMO, Ojima DS, Gilmanov TG, Scholes RJ, Schimel DS, Kirchner T, Menaut J-C, Seastedt T, Garcia Moya E, Kamnalrut A & Kinyamario JI (1993) Observations and modeling of biomass on soil organic matter dynamics for the grassland biome worldwide. Global Biogeochemical Cycles 7: 785–810

Prescott CE, Corbin JP & Parkinson D (1989) Biomass, productivity, and nutrient use efficiency of aboveground vegetation in four Rocky Mountain coniferous forests. Can. J. For. Res. 19: 309–317

Rehder H (1976) Nutrient turnover in alpine ecosystems. I. Phytomass and nutrient relations in four mat communities in the northern calcareous Alps. Oecologia 22: 411–423

Rehder H & Schafer A (1978) Nutrient studies in alpine ecosystems IV. Communities of the Central Alps and comparative survey. Oecologia 34: 309–327

Sanford Jr. RL, Parton WJ, Ojima DS & Lodge DJ (1991) Hurricane effects on soil organic matter dynamics and forest production in the Luqillo Experimental Forest, Puerto Rico: results of simulation modeling. BioTropica 23: 364–372

Sievering H, Burton D & Caine N (1992) Atmospheric loading of nitrogen to alpine tundra in the Colorado Front Range. Global Biogeochem. Cycles 6: 339–346

Spaulding SA (1991) Phytoplankton dynamics under ice-cover in a subalpine lake. M.S. Thesis, Colorado State University, Fort Collins

Stoddard JL (1991) Trends in Catskill stream water quality: evidence from historical data. Water Resour. Res. 27: 2855–2864

Stoddard JL (1994) Long-term changes in watershed retention of nitrogen: its causes and consequences. In: Baker LA (Ed) Environment chemistry of lakes and reservoirs. Advances in Chemistry Series No. 237. American Chemical Society, Washington DC

SYSTAT: Statistics, Version 5.2 Edition (1992). SYSTAT Inc., Evanston, Illinois.

Vitousek PM & Howarth RW (1991) Nitrogen limitation on land and in the sea: how can it occur? Biogeochemistry 13: 87–116

Vogt KA, Grier CC & Vogt DJ (1986) Production, turnover, and nutrient dynamics of above- and belowground detritus of world forests. Adv. Ecol. Res. 15: 303–377

Walthall PM (1985) Acidic deposition and the soil environment of Loch Vale Watershed in Rocky Mountain National Park. Ph.D. Dissertation, Colorado State University, Fort Collins

Webber PJ & May DE (1977) The magnitude and distribution of belowground plant structures in the alpine tundra of Niwot Ridge, Colorado. Arctic Alp. Res. 9: 157–174

Williams MW & Melack JM (1991) Precipitation chemistry in and ionic loading to an alpine basin, Sierra Nevada. Wat. Resour. Res. 27: 1563–1574

Williams MW, Brown AD & Melack JM (1993) Geochemical and hydrologic controls on the composition of surface water in a high-elevation basin, Sierra Nevada, California. Limnol. Oceanogr. 38: 775–797